

Supplementary Material

Table S1. Cyclic heptapeptides in the sponge *Styliissa caribica*.

Table S2. Full NMR data of stylissamide L (**1**) (^1H 700 MHz, ^{13}C 175 MHz, DMSO- d_6).

Table S3. Links to LC-MS data and molecular networks.

Figure S1. Molecular networks obtained using (a) the program MetGem (b) the Metabolomics workflow on GNPS, and (g) the Feature-Based Molecular Network workflow on GNPS.

Figure S2. Positive ion mode high-resolution ESI mass spectrum of stylissamide L (**1**).

Figure S3. Positive ion mode high-resolution ESI MS/MS spectrum of stylissamide L (**1**).

Figure S4. ^1H -NMR spectrum of stylissamide L (**1**) (700 MHz, DMSO- d_6).

Figure S5. ^{13}C -NMR spectrum of stylissamide L (**1**) (175 MHz, DMSO- d_6).

Figure S6. COSY spectrum of stylissamide L (**1**) (700 MHz, DMSO- d_6).

Figure S7. TOCSY spectrum of stylissamide L (**1**) (700 MHz, DMSO- d_6).

Figure S8. Spin systems of stylissamide L (**1**) from the sections of the TOCSY spectrum.

Figure S9. NOESY spectrum of stylissamide L (**1**) (700 MHz, DMSO- d_6).

Figure S10. HSQC spectrum of stylissamide L (**1**) (700 MHz, DMSO- d_6).

Figure S11. HMBC spectrum of stylissamide L (**1**) (700 MHz, DMSO- d_6).

Figure S12. Band-selective HMBC spectrum of stylissamide L (**1**) (700 MHz, DMSO- d_6).

Figure S13. UV and ECD spectra of stylissamide L (**1**) in ACN.

Figure S14. Real time monitoring of cancer cell proliferation after exposure to stylissamide L (**1**).

Figure S15. Real-time monitoring of 3AB-OS and MCF-7 cell migration after exposure to stylissamide L (**1**).

Table S1. Cyclic heptapeptides in the sponge *Styliissa caribica*.

Cyclic peptide	[M+H] ⁺	Exact Mass	Retention time RP-18 ^a	Retention time PFP ^b	Citation
Styliissamide A	C ₄₄ H ₆₁ N ₈ O ₉	845.4556	1.72	26.34	c,d,e
Styliissamide B	C ₄₄ H ₅₈ N ₇ O ₈	812.4341	ND	ND	c,d,e
Styliissamide C	C ₄₈ H ₆₀ N ₇ O ₈	862.4498	20.29	32.66	c,d,e
Styliissamide D	C ₄₅ H ₆₂ N ₇ O ₈	828.4654	19.55	32.48	c,d,e
Styliissamide E	C ₃₉ H ₅₉ N ₈ O ₉	783.4400	13.29	28.76	d,e
Styliissamide F	C ₄₃ H ₅₇ N ₁₀ O ₉	857.4304	13.94	32.21	d,e
Styliissamide G	C ₄₅ H ₆₂ N ₇ O ₇	812.4705	ND	ND	e
Styliissamide H	C ₄₄ H ₅₉ N ₈ O ₈	827.4450	ND	ND	e
Styliissamide L	C ₄₁ H ₅₃ N ₈ O ₁₀	817.3876	6.21	24.95	this work
Hymenamide C	C ₄₃ H ₅₅ N ₈ O ₉	827.4087	20.71	32.58	f
Hymenamide F	C ₃₅ H ₆₁ N ₁₀ O ₈ S	781.4389	1.67	26.40	f
Phakellistatin 3	C ₄₂ H ₅₅ N ₈ O ₉	815.4087	18.50	31.89	h
Phakellistatin 13	C ₄₂ H ₅₅ N ₈ O ₈	799.4137	20.09	32.47	g
Stylisin 1	C ₄₅ H ₆₂ N ₇ O ₈	828.4654	ND	ND	c,d,e,g
Stylisin 2	C ₄₄ H ₅₈ N ₇ O ₈	812.4341	ND	ND	c,d,e,g

- a. Experiments were performed with a Kinetex 5 μm , 50 mm \times 2.10 mm C18 column using a flow rate of 200 $\mu\text{L}/\text{min}$ and the following elution gradient: 10% MeOH for 1 min, 10%–100% MeOH over 30 min, and 100% MeOH for 10 min.
- b. Experiments were performed with a Kinetex 5 μm , 100 mm \times 2.1 mm PFP column using a flow rate of 200 $\mu\text{L}/\text{min}$ and the same elution gradient of H₂O and MeOH described above.
- c. Schmidt, G.; Grube, A.; Köck, M. Styliissamides A-D - New proline-containing cyclic heptapeptides from the marine sponge *Styliissa caribica*. European J. Org. Chem. 2007, 2, 4103–4110, doi:10.1002/ejoc.200700013.
- d. Cychon C.; Köck, M. Styliissamides E and F, Cyclic Heptapeptides from the Caribbean Sponge *Styliissa caribica*. J. Nat. Prod. 2010, 73, 738–742, doi: 10.1021/np900664f.
- e. Wang, X.; Morinaka, B. I.; Molinski, T. F. Structures and solution conformational dynamics of styliissamides G and H from the Bahamian Sponge *Styliissa caribica*. J. Nat. Prod. 2014, 77, 625–630, doi:10.1021/np400891s.
- f. Grube, A.; Maier, T.; Köck, M. MS-guided Fractionation as a Fast Way to the Identification of New Natural Products – MALDI-TOF-MS Screening of the Marine Sponge *Styliissa caribica*. Zeitschrift für Naturforsch. B 2007, 62, 600–604, doi:10.1515/znb-2007-0420..
- g. Mohammed, R.; Peng, J.; Kelly, M.; Hamann, M.T. Cyclic heptapeptides from the Jamaican sponge *Styliissa caribica*. J. Nat. Prod. 2006, 69, 1739–1744, doi:10.1021/np060006n.
- h. This compound was not previously detected in specimens of *Styliissa caribica*. It was putatively identified by the Dereplicator tool in GNPS.

Table S2. Full NMR data of stylissamide L (1) (^1H 700 MHz, ^{13}C 175 MHz, DMSO- d_6).

AA	pos.	δ_{C} , type	δ_{H} , mult (J in Hz)	NOESY	HMBC
Pro ^I	1	170.3, C	-		
	2	59.1, CH	4.34, dd (5.1, 8.6)	Ser-NH, Tyr-NH, Phe-NH	Phe-1
	3	28.1, CH ₂	a 2.15, m b 1.75, m	Pro ^{II} -4b, Pro ^{II} -3a Pro ^{II} -2, Pro ^{II} -4b	Pro ^I -1 Pro ^I -1
	4	24.3, CH ₂	1.87, m		
	5	46.7, CH ₂	a 3.45, m b 3.36, m		Pro ^I -1
					Phe-1, Pro ^I -2
Pro ^{II}	1	171.8, C	-		
	2	60.1, CH	4.28, dd (1.5, 8.8)	Ser-NH, Pro ^I -2, Pro ^I -3b	Pro ^{II} -1, Pro ^{II} -5
	3	31.8, CH ₂	a 2.16, m b 2.00, m	Ser-NH	Pro ^{II} -1
	4	21.7, CH ₂	a 1.77, m b 1.57, m	Pro ^{III} -3a	
	5	46.8, CH ₂	a 3.60, ddd (1.5, 8.4, 10.8) b 3.33, ddd (10.8, 10.8, 7.1)	Ser-NH Pro ^{III} -4b	Pro ^I -1
			7.65, d (5.9)	Tyr-NH, Pro ^I -2, Pro ^{II} -2, Pro ^{II} -5a, Pro ^{II} -4b	Pro ^{II} -1
Ser	NH				
	1	167.7, C	-		
	2	60.0, CH	3.85, ddd (3.6, 5.9, 10.2)	Tyr-NH	Ser -1
	3	60.9, CH ₂	a 3.46, dd (10.2, 11.9) b 3.14, dd (11.9, 3.6)	Tyr-NH, Tyr-5/9	
			7.34, d (9.1)	Ser-NH, Ser-3a	Ser-1
Tyr	NH	171.5 C	-		
	1	51.5 CH	4.88 ddd (3.2, 9.1, 10.9)	Pro ^{III} -5a/b	Tyr- 1
	2	37.0 CH ₂	a 3.35, dd (3.2, 13.5) b 2.42, dd (10.9, 13.5)	Pro ^{III} -5a/b, Phe-NH, Gln-NH Gln-NH, Phe-NH, Pro ^{III} -5a	Tyr-5/9 Tyr-1, Tyr-4
	4	126.6 C	-		
	5/9	130.5 CH	7.08, d (8.5)	Tyr-3a, Tyr-3b	Tyr-7
	6/8	114.9 CH	6.66, d (8.5)		Tyr-7
Pro ^{III}	7	156.0 C	-		
	7-OH		7.42, s		
	1	171.9, C	-		
	2	63.1, CH	4.06, t (8.7)	Phe-NH,	Pro ^{III} -1
	3	28.7, CH ₂	a 2.22 m b 1.81, m	Gln-NH	Pro ^{III} - 1
	4	25.0, CH ₂	a 2.11, m b 1.98, m	Gln-NH, Gln-3a, Gln-3b	
Gln	NH	46.9, CH ₂	a 3.93, ddd (6.8, 9.8, 9.8) b 3.82, m	Tyr-2, Tyr-3a Tyr-2, Gln-NH, Tyr-3a	Pro ^{III} -3
			8.17, d (7.0)	Phe-NH, Tyr-3a, Pro ^{III} -2, Pro ^{III} -3b, Pro ^{III} -4a	Pro ^{III} -1
	1	170.7, C	-		
	2	52.8, CH	4.05, ddd (4.3, 7.0, 10.0)	Phe-NH, Pro ^{III} -4b	Gln-1
	3	25.9, CH ₂	a 1.85, m b 1.73, m	Pro ^{III} -4a Pro ^{III} - 4a	Gln-1, Gln-5 Gln-5
	4	31.5, CH ₂	a 2.13, ddd (7.2, 15.7, 7.2) b 2.04, ddd (7.2, 15.7, 7.2)	Pro ^{III} -5b, Pro ^{III} -3a, Pro ^{III} -3b Pro ^{III} -4a	Gln-5 Gln-5
Phe	5	174.5, C	-		
	5-NH ₂		6.92, s	Gln-4a, Gln-4b	Gln-5
	NH		7.11, d (7.2)	Phe-2, Gln-NH, Pro ^{III} -2, Pro ^I -5b, Tyr-NH	Gln-1
	1	167.5 C	-		
	2	51.5, CH	4.69, ddd (5.8, 7.2, 8.0)	Pro ^I -5a, Pro ^I -5b	Phe-1, Phe-4
	3	36.9 CH ₂	a 3.18, dd (8.0, 14.2) b 2.71 (5.8, 14.2)		Phe-1, Phe-4 Phe-1, Phe-5/9
	4	138.0, C	-		
	5/9	128.9, CH	7.16, d (7.5)		
	6/8	126.0, CH	7.18, t (7.3)		
	7	128.0, CH	7.22, t (7.5)		

Table S3. Links to LC-MS data and molecular networks.

Description	Link
Classical Molecular Networking (Metabolomics) workflow	https://gnps.ucsd.edu/ProteoSAFe/status.jsp?task=4acb49028d7041c39fccf03dd6e8c195
Feature-Based Molecular Networking workflow	https://gnps.ucsd.edu/ProteoSAFe/status.jsp?task=db7aa9e8bec64d6290cc040254f00b87
Dereplicator	https://gnps.ucsd.edu/ProteoSAFe/status.jsp?task=f8b123b5ea89494481549c1a519caf5d
LC-MS data on Massive	https://massive.ucsd.edu/ProteoSAFe/dataset.jsp?task=f77c49cb5d73489583c08d3e66b558e1 FTP access: ftp://MSV000085904@massive.ucsd.edu password: Sty_reviewers

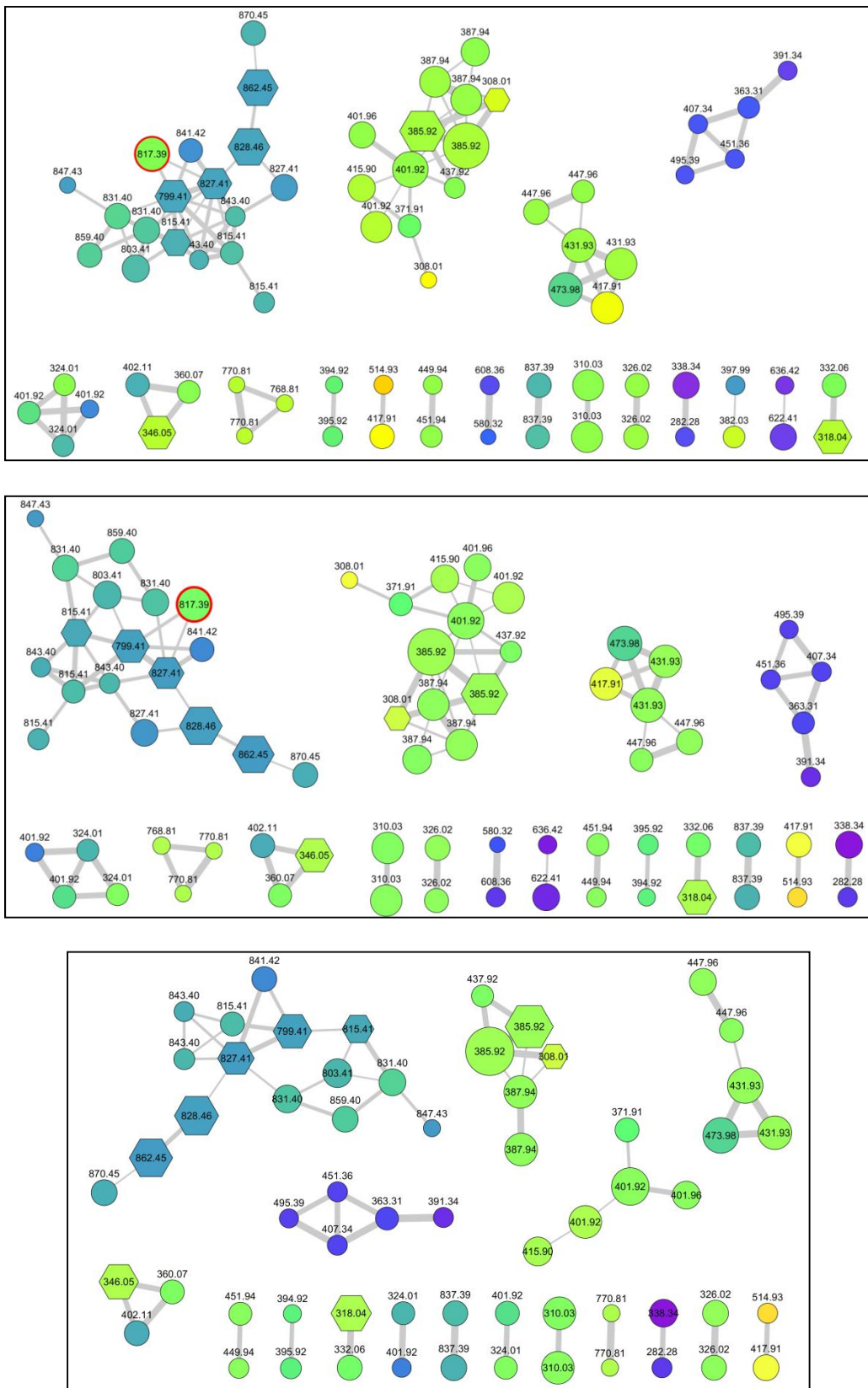


Figure S1. Molecular networks of the extract of *S. caribica* obtained with the same data and the same parameters (m/z tolerance 0.01 Da, cosine score > 0.55 , matched peaks > 8 , maximum number of neighbor nodes = 10) using (a) the program MetGem (b) the Metabolomics workflow on GNPS, and (c) the Feature-Based Molecular Network workflow on GNPS.

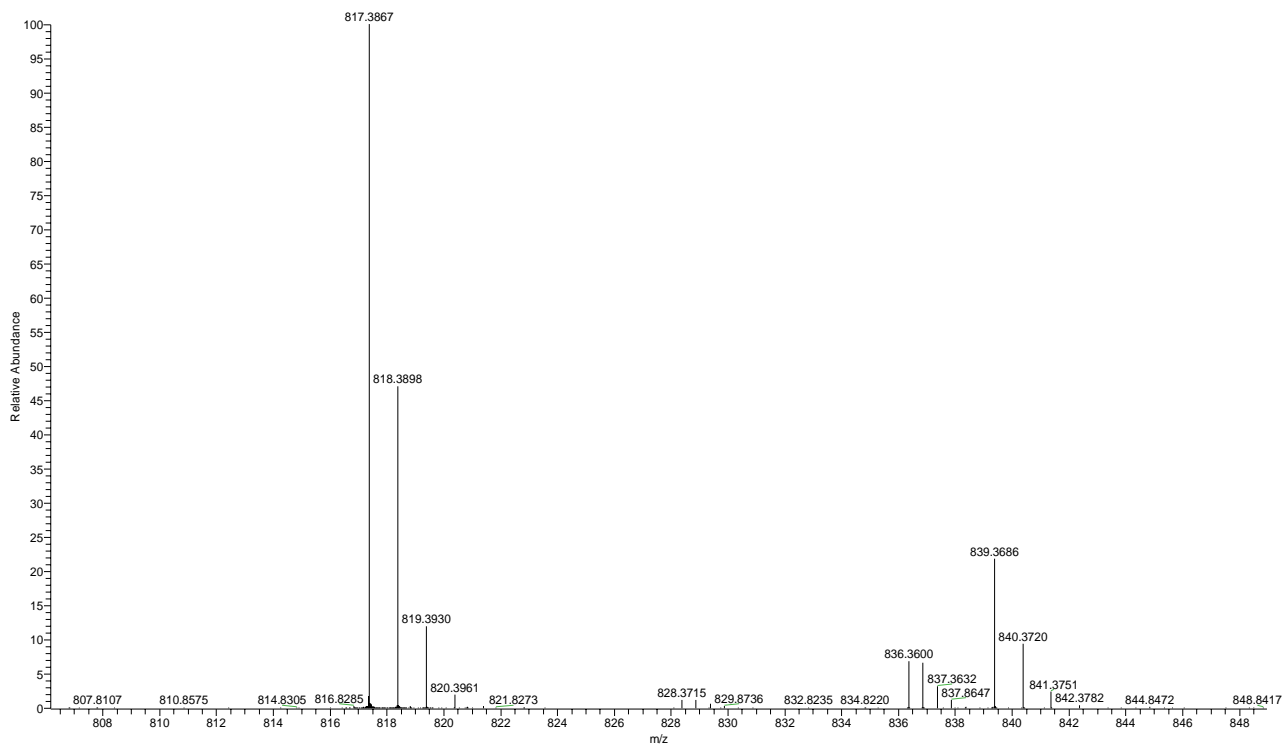


Figure S2. Positive ion mode high-resolution ESI mass spectrum of stylissamide L (1).

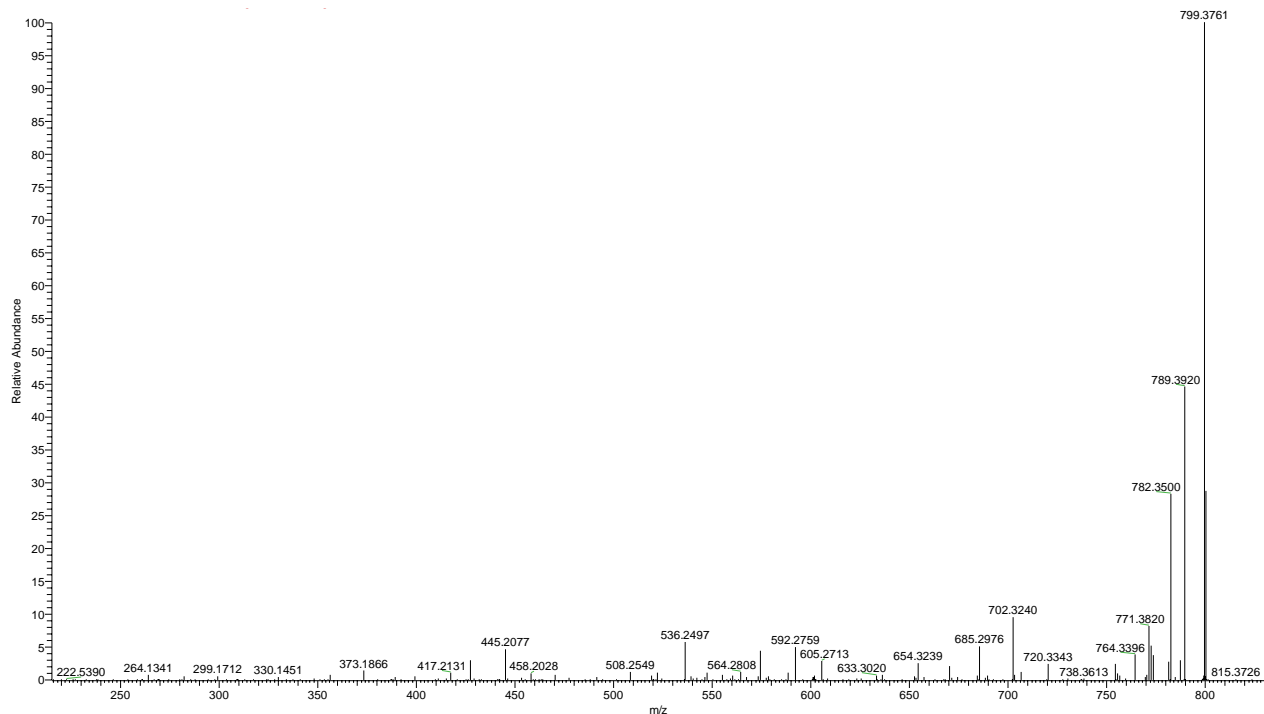


Figure S3. Positive ion mode high-resolution ESI MS/MS spectrum of stylissamide L (1).

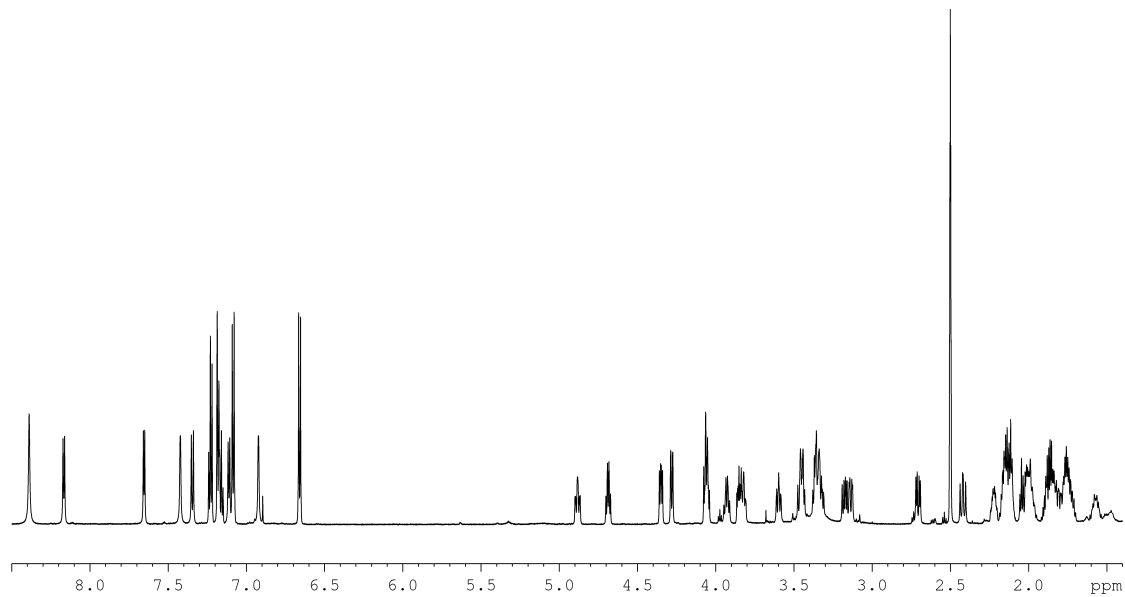


Figure S4. ¹H-NMR spectrum of stylissamide L (1) (700 MHz, DMSO-*d*₆).

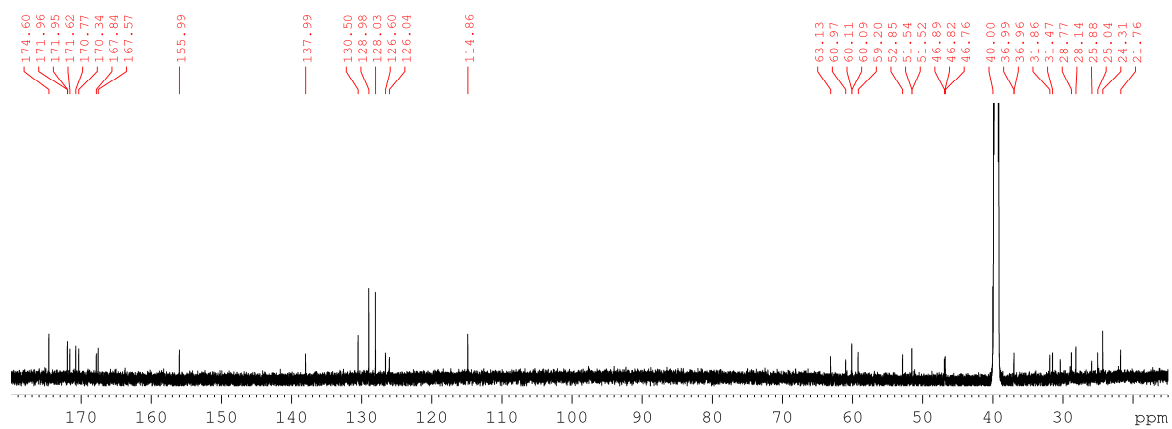


Figure S5. ¹³C-NMR spectrum of stylissamide L (1) (175 MHz, DMSO-*d*₆).

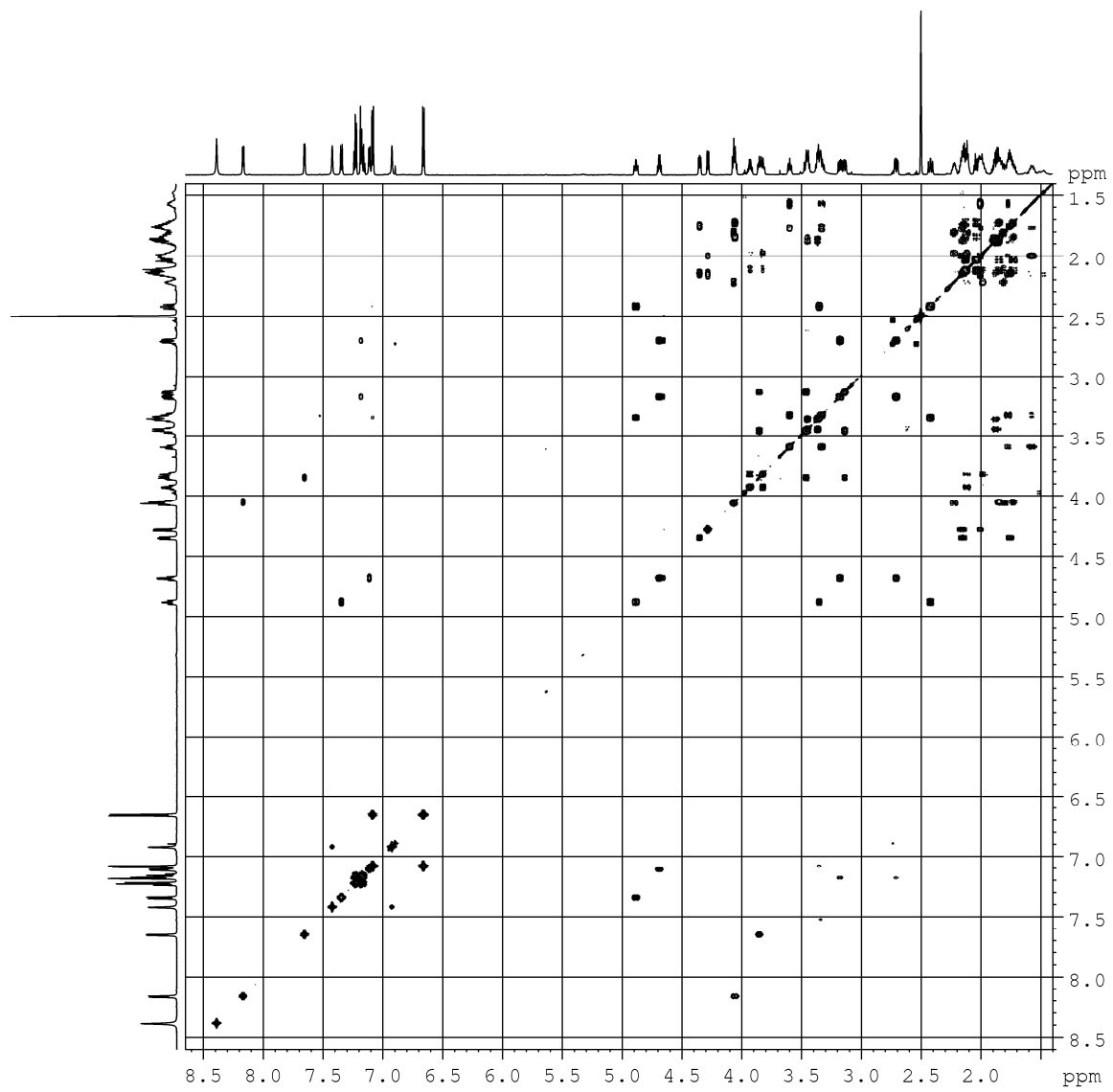


Figure S6. COSY spectrum of stylissamide L (1) (700 MHz, $\text{DMSO}-d_6$).

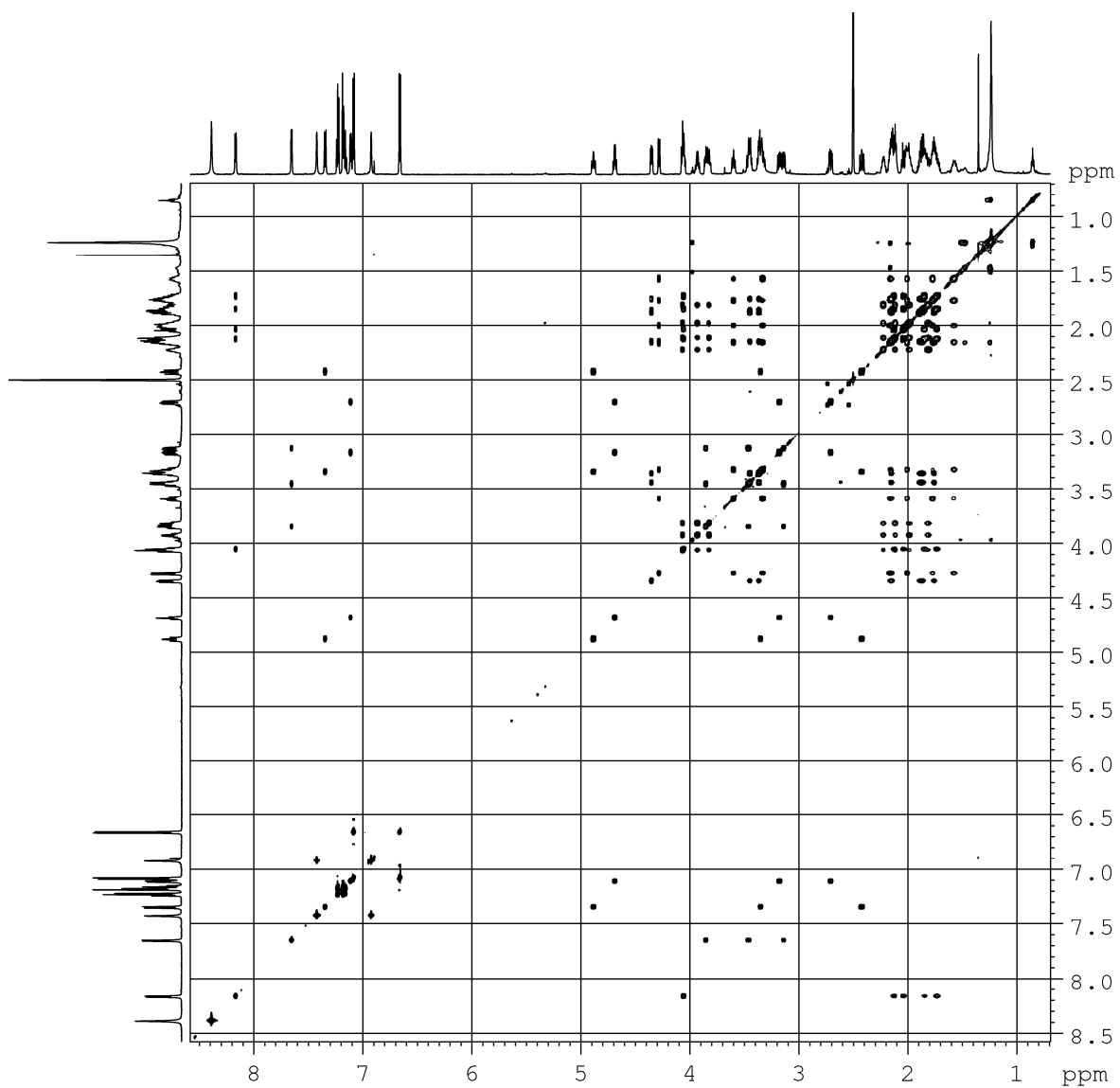


Figure S7. TOCSY spectrum of stylissamide L (1) (700 MHz, $\text{DMSO}-d_6$).

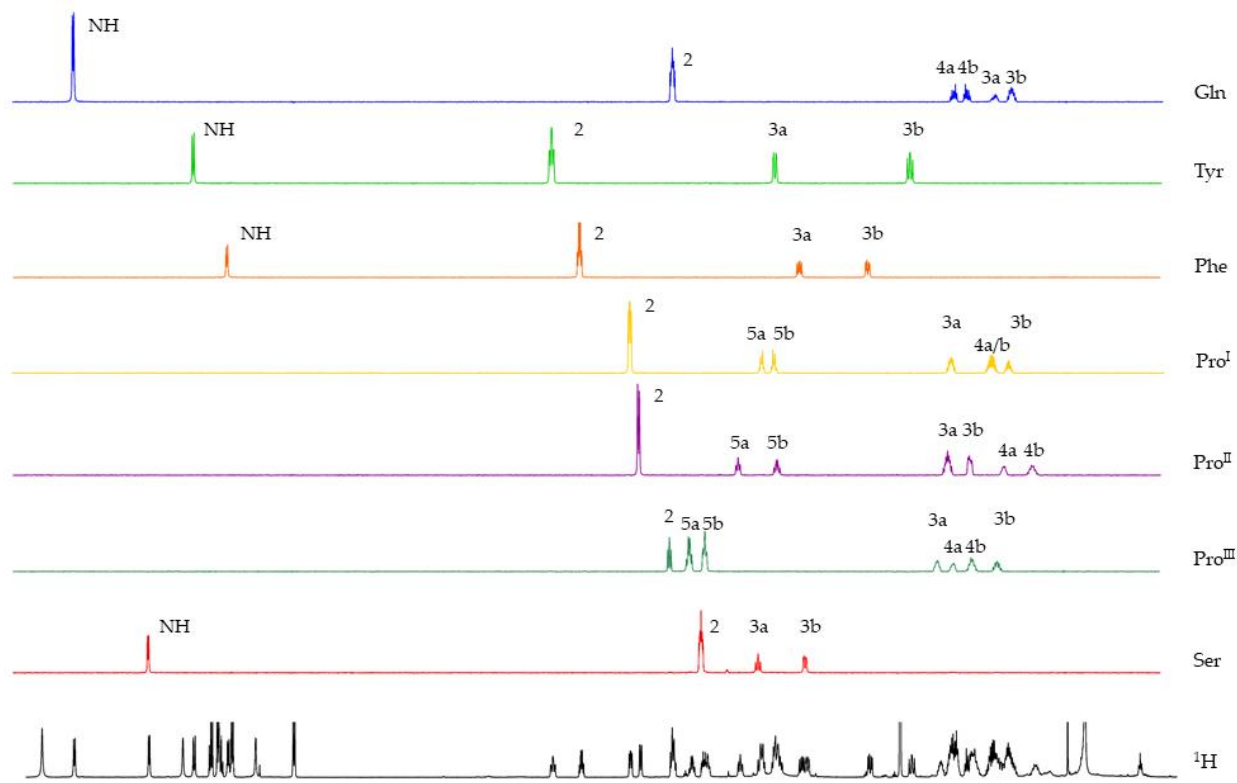


Figure S8. Spin systems of stylissamide L (1) from the sections of the TOCSY spectrum.

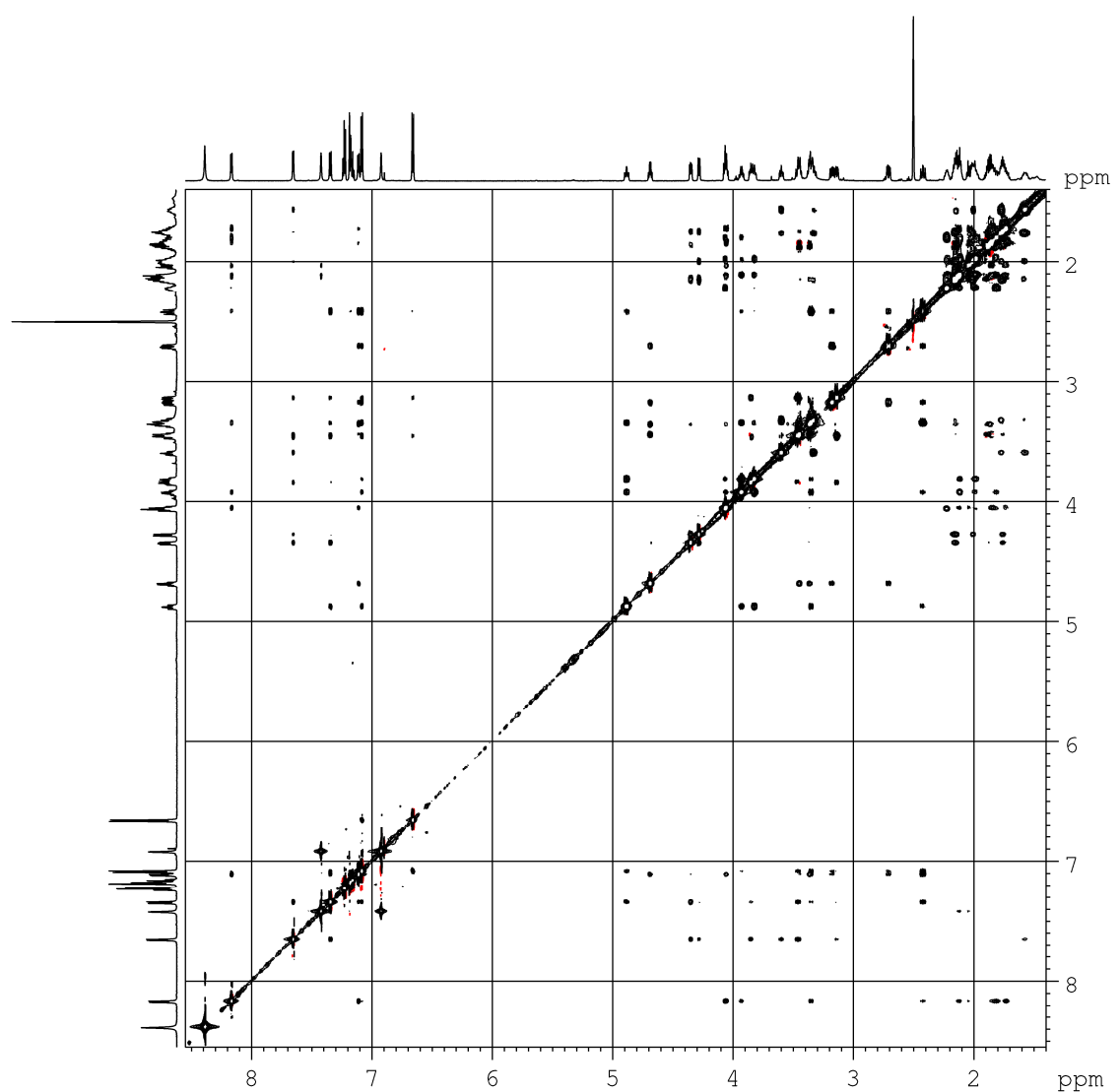


Figure S9. NOESY spectrum of stylissamide L (1) (700 MHz, $\text{DMSO}-d_6$).

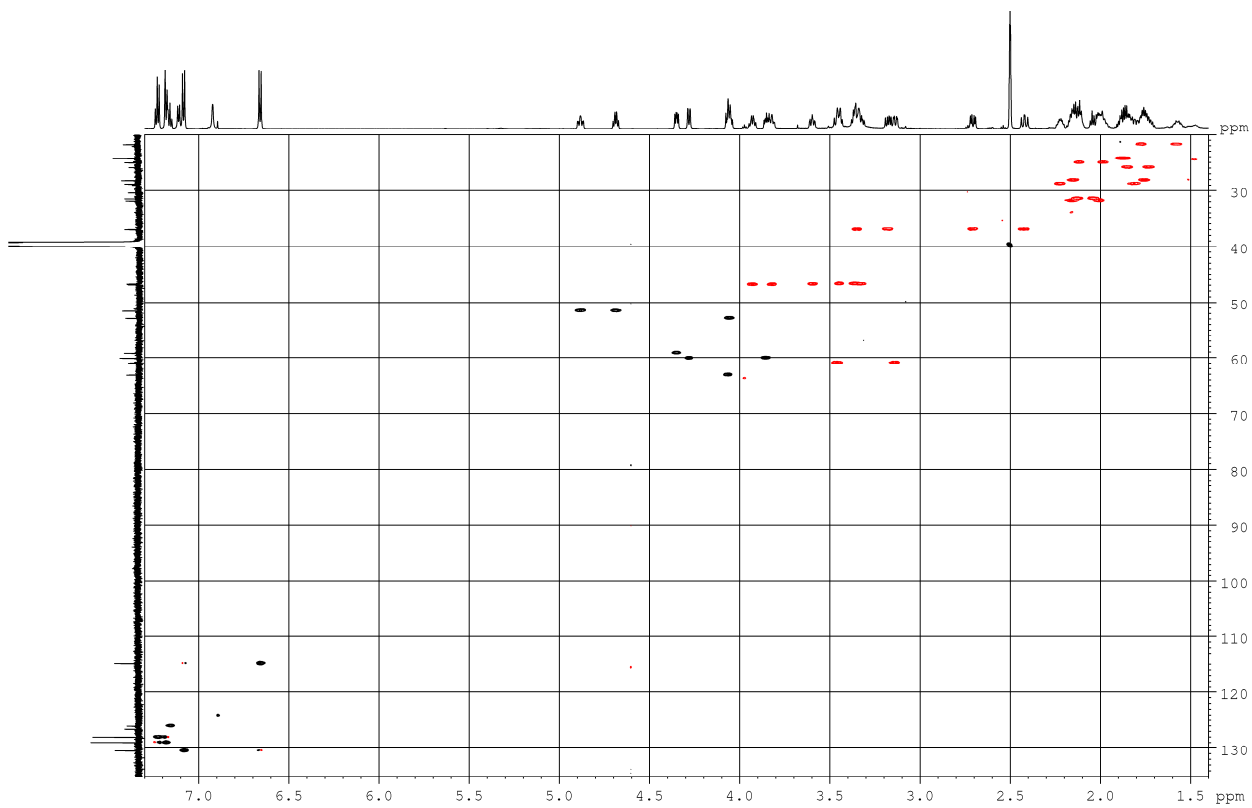


Figure S10. HSQC spectrum of stylissamide L (1) (700 MHz, $\text{DMSO}-d_6$).

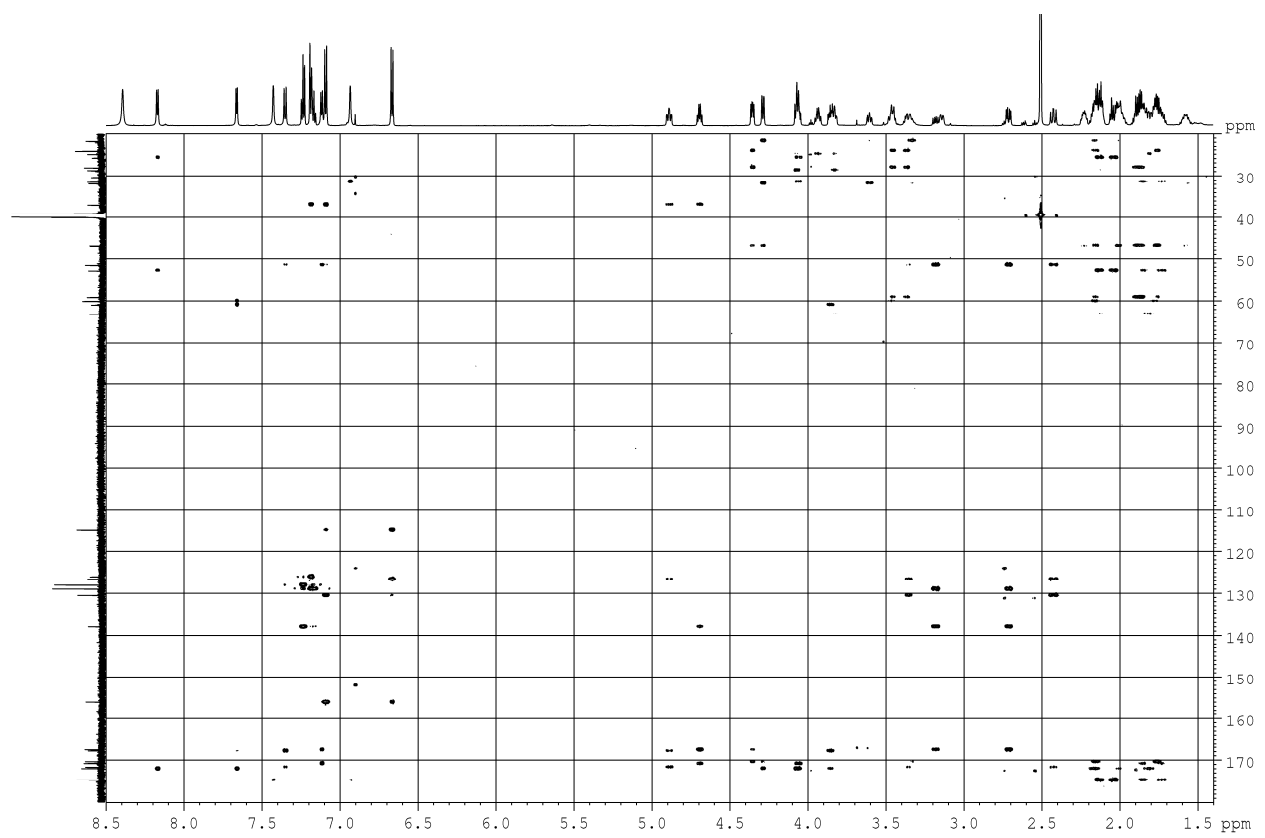


Figure S11. HMBC spectrum of stylissamide L (1) (700 MHz, $\text{DMSO}-d_6$).

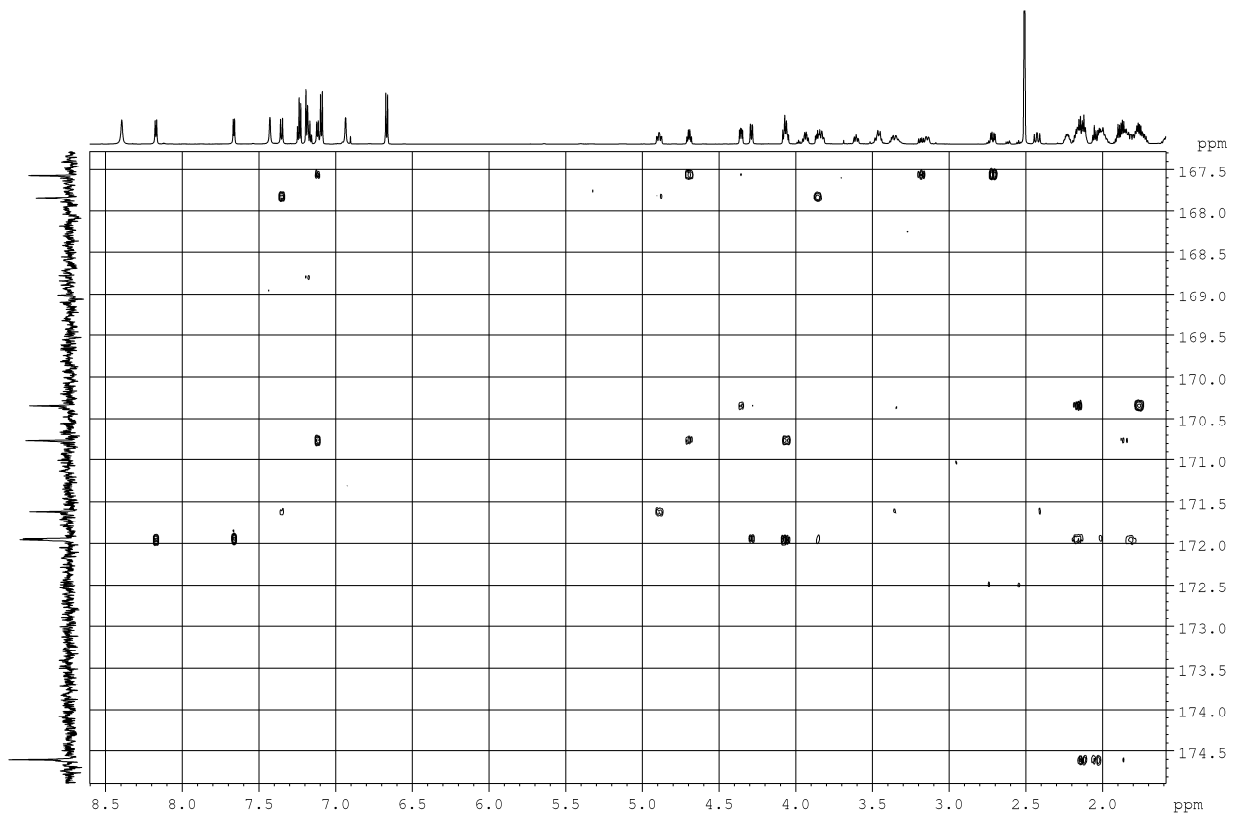


Figure S12. Band-selective HMBC spectrum of stylissamide L (1) (700 MHz, DMSO-*d*₆).

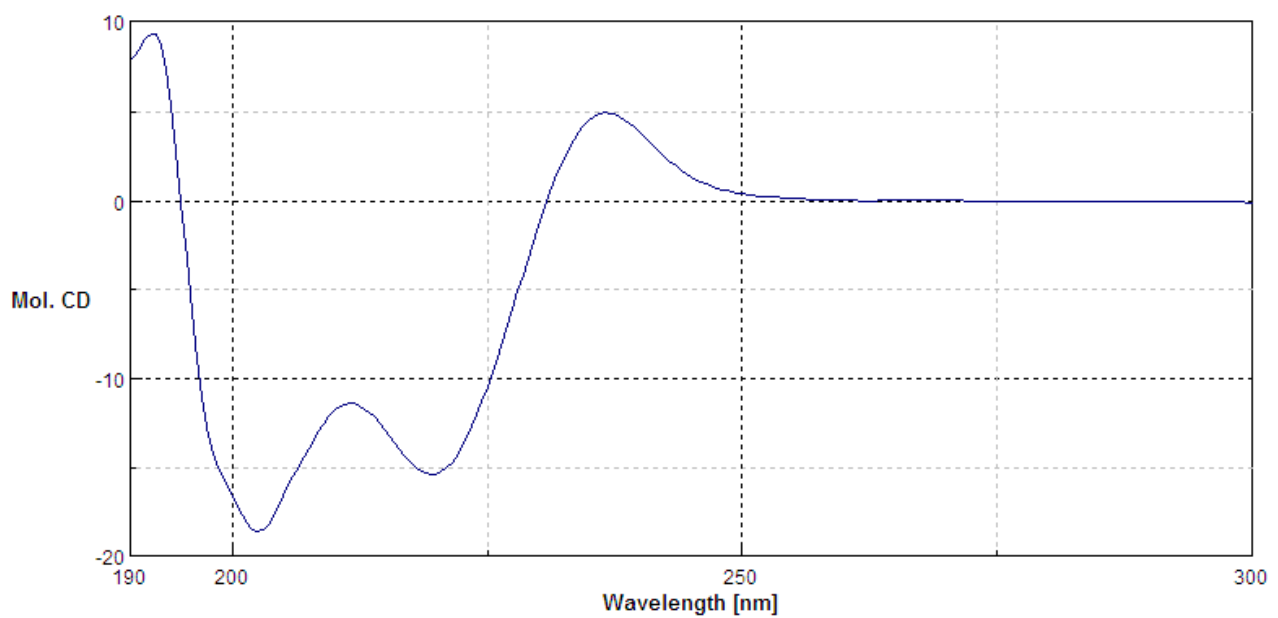
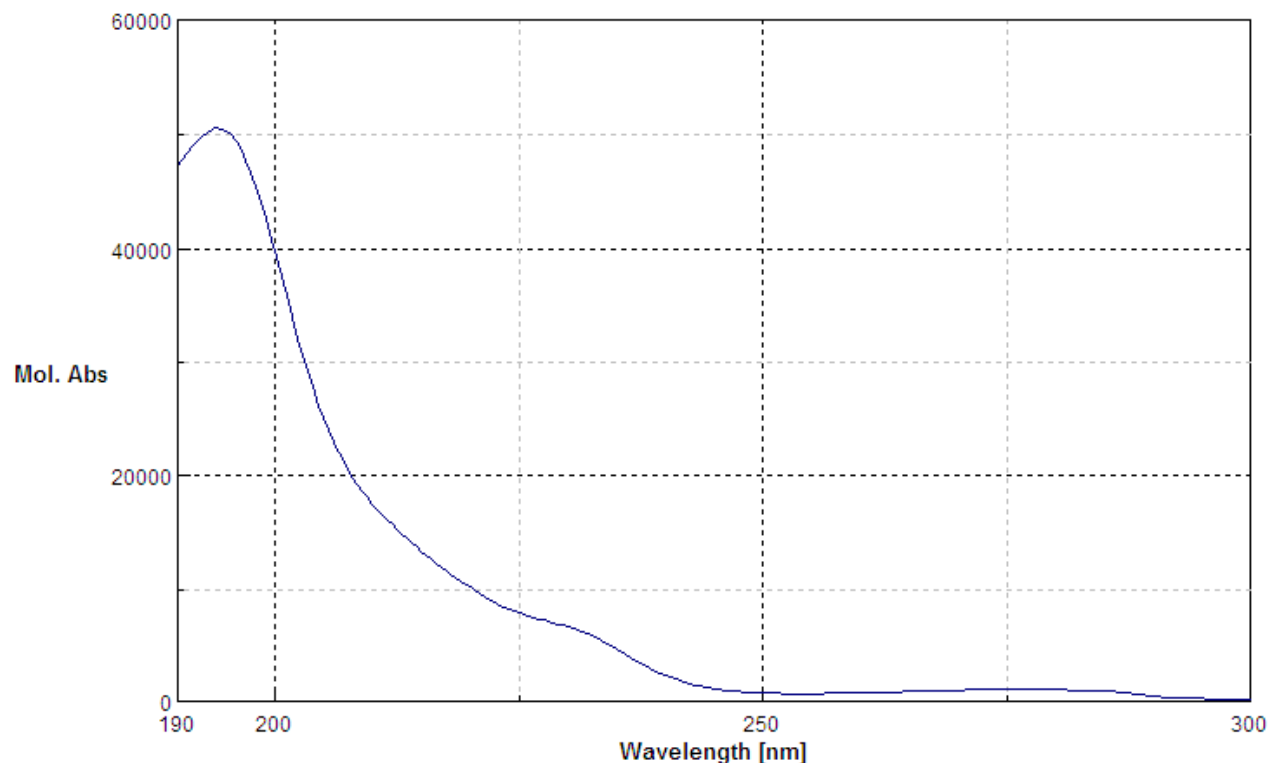


Figure S13. UV and ECD spectra of stylissamide L (1) in ACN.

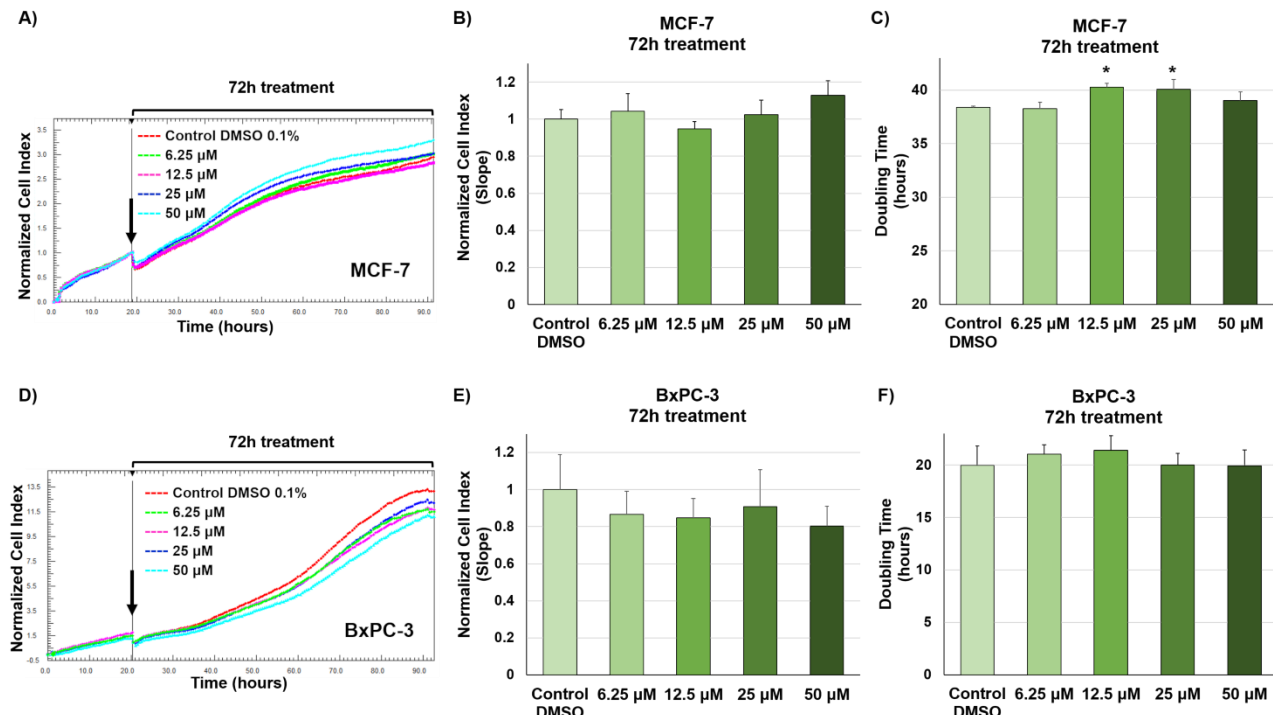


Figure S14. Real time monitoring of cancer cell proliferation after exposure to stylissamide L (**1**) and DMSO vehicle, by using the xCELLigence System Real-Time Cell Analyzer. **(A,D)** Normalized cell index (NCI) traces of MCF7 (**A**) and BxPC-3 (**D**) cells treated with different concentrations (6.25, 12.5, 25, and 50 µM) of stylissamide L (**1**) and DMSO vehicle (0.1%) for 72 hours. Black arrow shows the start of drug treatment. Each cell index value was normalized at this time. **(B,E)** Slope values of growth curves of MCF-7 (**B**) and BxPC-3 (**E**) cells after 72 h exposure to different concentrations (6.25, 12.5, 25, and 50 µM) of stylissamide L (**1**) and DMSO vehicle (0.1%). NCI slope values are relative to controls treated with DMSO vehicle. **(C,F)** Doubling times of NCI of MCF-7 (**C**) and BxPC-3 (**F**) cells after 72 h treatment with different concentrations (6.25, 12.5, 25, and 50 µM) of stylissamide L (**1**) and DMSO (0.1%). Data are presented as mean ± SD; n=3. Statistical significances are referred to the DMSO control. One-way analysis of variance (ANOVA) was applied to compare means of groups and Dunnett's method was used as a post-hoc test to compare multiple groups versus the control group. *p*-values < 0.05 were considered to be statistically significant. Statistical analysis was performed using the GraphPad Prism Software Version 5. * *p* < 0.05.

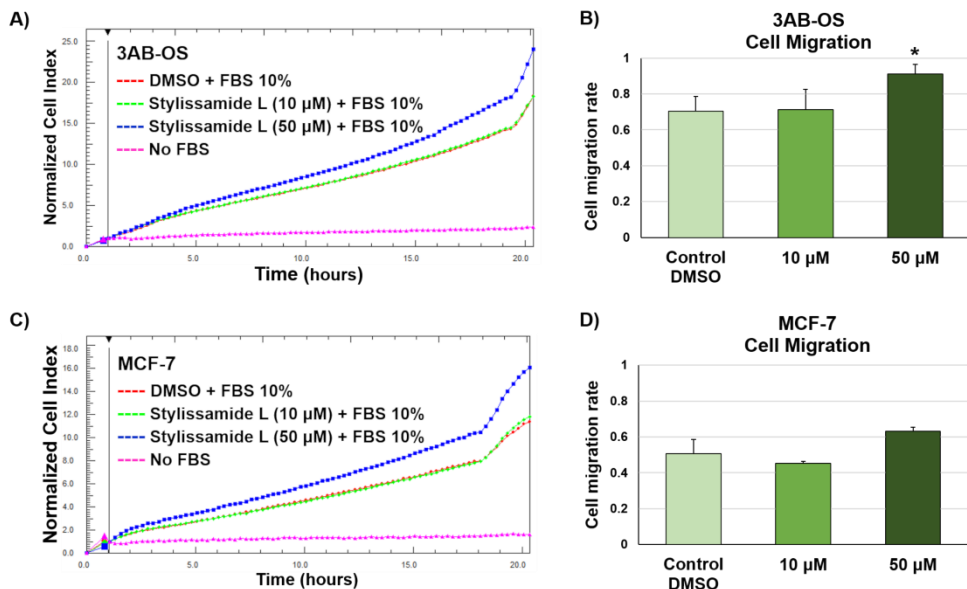


Figure S15. Real-time monitoring of 3AB-OS and MCF-7 cell migration after exposure to stylissamide L (**1**). (A,C) NCI traces of 3AB-OS (A) and MCF-7 (C) cells seeded with compound **1** or DMSO (0.1%) vehicle, in presence of 10% Fetal Bovine Serum (FBS) as the chemoattractant. Migration was monitored for 20 hours, using the xCELLigence System equipped with specially designed 16-well plates (CIM-plate 16). (B,D) Migration activity of 3AB-OS (B) and MCF-7 (D) cells seeded with compound **1** or DMSO (0.1%) vehicle, in presence of 10% Fetal Bovine Serum (FBS) as the chemoattractant. Cell migration rates were recorded for 20 hours and expressed as slope values of NCI curves. Data are presented as mean \pm SD; n=3. Statistical significances are referred to the DMSO control. Two-group comparisons were performed using Student's t-test. P-values < 0.05 were considered to be statistically significant. Statistical analysis was performed using the GraphPad Prism Software Version 5.